

See discussions, stats, and author profiles for this publication at: <https://www.researchgate.net/publication/230795801>

Si(6-n)C(n)H(6) (n = 0-6) Series: When Do Silabenzenes Become Planar and Global Minima?

ARTICLE *in* THE JOURNAL OF PHYSICAL CHEMISTRY A · SEPTEMBER 2012

Impact Factor: 2.69 · DOI: 10.1021/jp307722q · Source: PubMed

CITATIONS

21

READS

58

2 AUTHORS:



Alexander Ivanov

Oak Ridge National Laboratory

24 PUBLICATIONS 130 CITATIONS

[SEE PROFILE](#)



Alexander I Boldyrev

Utah State University

341 PUBLICATIONS 9,952 CITATIONS

[SEE PROFILE](#)

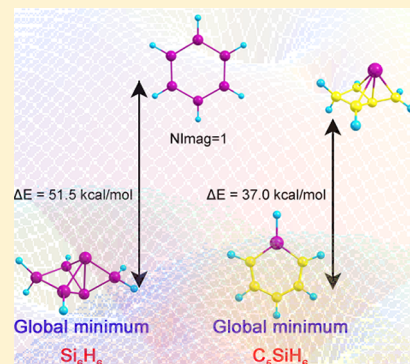
$\text{Si}_{6-n}\text{C}_n\text{H}_6$ ($n = 0-6$) Series: When Do Silabenzenes Become Planar and Global Minima?

Alexander S. Ivanov and Alexander I. Boldyrev*

Department of Chemistry and Biochemistry, Utah State University, 0300 Old Main Hill, Logan, Utah 84322, United States

S Supporting Information

ABSTRACT: In the current work we studied a structural transition from nonplanar three-dimensional structures to planar benzene-like structures in the $\text{Si}_{6-n}\text{C}_n\text{H}_6$ ($n = 0-6$) series. We performed unbiased Coalescence–Kick global minimum and low-lying isomers search for the Si_6H_6 , Si_5CH_6 , $\text{Si}_4\text{C}_2\text{H}_6$, $\text{Si}_3\text{C}_3\text{H}_6$, $\text{Si}_2\text{C}_4\text{H}_6$, and SiC_5H_6 stoichiometries at the B3LYP/6-31G** level of theory. The lowest isomers were recalculated at the CCSD(T)/CBS//B3LYP/6-311++G** level of theory. It was shown that the pseudo-Jahn–Teller effect, which is responsible for the deformation of planar Si_6H_6 , Si_5CH_6 , and $\text{Si}_4\text{C}_2\text{H}_6$ structures, is suppressed at $n = 3$ (the planar structure of 1,3,5-trisilabenzene). We also showed that the 3D–2D transition, which occurs only at $n = 5$, is due to the aromaticity of monosilabenzene (SiC_5H_6) along with other factors, such as stronger C–C σ bonds compared to weaker C–Si and Si–Si σ bonds.



INTRODUCTION

Silicon and carbon are both in the fourth column of the Periodic Table; however, structures and properties of their compounds are very different. As for hydrocarbons with C_6H_6 stoichiometry, the aromatic benzene molecule is by far the lowest-energy structure, with benzvalene and prismane being more than 70 kcal/mol higher.¹ Silicon hydrides Si_xH_y , contrary to hydrocarbons, are usually characterized by electron-poor bonds,^{2–5} weaker π – π interaction,^{6,7} and even the hydrocarbon analogs satisfying the octet rule are not the most stable isomers on the potential energy surface (PES) of Si_xH_y .^{8–12} In spite of that, the question regarding the possibility of planar benzene-like silicon analogs has been addressed long ago^{13,14} and it continues to be the subject of research nowadays.^{15,16} Hexasilabenzene (structure I.33, Figure 1) has been studied considerably^{14,17} as a molecule analogous to benzene, and its aromaticity has also been discussed.¹⁸ It is turned out that the D_{6h} hexasilabenzene structure I.33 is not even a local minimum, but a first-order saddle point. Geometry optimization along the imaginary mode leads to the distorted nonplanar chairlike structure I.32 (D_{3d} , $^1\text{A}_{1g}$).¹⁴ According to the present calculations at CCSD(T)/CBS//B3LYP/6-311++G**, chairlike structure I.32 (Figure 1) is 51.4 kcal/mol higher than the global minimum structure I.1 and 20.7 kcal/mol higher than prismane I.18, which has been considered as the global minimum structure of Si_6H_6 for almost thirty years.^{13,17,19} It was recently shown that prismane is just a local minimum on the Si_6H_6 PES and structure I.1 is the global minimum for Si_6H_6 stoichiometry.²⁰ Structure I.1 was isolated and characterized in the form of aryl-substituted Si_6H_6 according to the latest experimental reports.²¹

A structural transition from the three-dimensional nonplanar structures to the two-dimensional planar benzene-like struc-

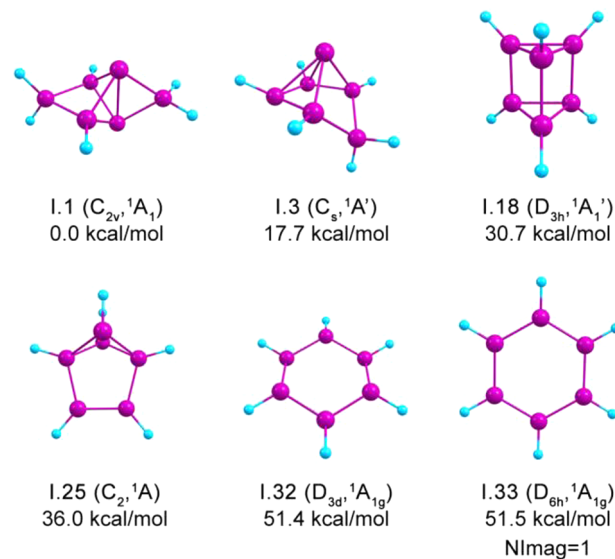


Figure 1. Selected lowest-energy structures of Si_6H_6 , their point group symmetries, spectroscopic states, and ZPE (B3LYP/6-311++G**) corrected relative energies (CCSD(T)/CBS//B3LYP/6-311++G**). The structures are labeled in accordance with Figure S1 (see Supporting Information).

tures is expected to occur in the $\text{Si}_{6-n}\text{C}_n\text{H}_6$ ($n = 0-6$) series upon sequential substitution of the Si atoms by C atoms. In this work we present a systematic study of $\text{Si}_{6-n}\text{C}_n\text{H}_6$ ($n = 0-6$) series and demonstrate that benzene-like structures become the

Received: August 3, 2012

Revised: August 22, 2012

Published: September 4, 2012



lowest energy isomers only at $n = 5$ (SiC_5H_6). The above-mentioned distortion of the D_{6h} hexasilabenzene Si_6H_6 was traced in the series also. We showed that the pseudo-Jahn–Teller (PJT) effect, which is responsible for such a distortion, is completely suppressed at $n = 3$ (the planar structure of 1,3,5-trisilabenzene $\text{Si}_3\text{C}_3\text{H}_6$).

■ COMPUTATIONAL AND THEORETICAL METHODS

A computational search for the global minima structures of Si_6H_6 , Si_5CH_6 , $\text{Si}_4\text{C}_2\text{H}_6$, $\text{Si}_3\text{C}_3\text{H}_6$, $\text{Si}_2\text{C}_4\text{H}_6$, and SiC_5H_6 stoichiometries was performed using the Coalescence Kick (CK) program written by Averkiev.²² In the CK method, a random structure is first checked for connectivity: if all atoms in the structure belong to one fragment, then the structure is considered as connected, and the Berny algorithm²³ for geometry optimization procedure is applied to it. However, in most cases, a randomly generated structure is fragmented; that is, the structure contains several fragments nonbonded with each other including cases with just one atom not being connected. In these cases, the coalescence procedure is applied to the fragmented structure—all of the fragments are pushed to the center of mass simultaneously. The magnitude of shift should be small enough so that atoms do not approach each other too closely but large enough so that the procedure converges in a reasonable amount of time. In the current version of the CK program, a 0.2 Å shift is used. The obtained structure is checked for connectivity again, and the procedure repeats. When two fragments approach each other close enough, they “coalesce” to form a new fragment, which will be pushed as a whole in the following steps. Obviously, at some point, all fragments are coalesced. This method does not deal with cases when, in a randomly generated structure, two atoms are too close to each other. To avoid this problem, the initial structures are generated in a very large box with all three linear dimensions being 4* (the sum of atomic covalent radii). Hence, usually an initially generated random structure consists of separated atoms as initial fragments. The current version of the program is designed for the global minimum searches of both single molecules of desired composition and complexes of molecules like solvated anions (e.g., $\text{SO}_4^{2-} \cdot 4\text{H}_2\text{O}$),^{24,25} where the initial geometry of each molecular unit is specified in the input file. In the latter case, the two molecular units of the complex are considered as connected in a fragment if the distances between two of their atoms are less than the sum of the corresponding van der Waals radii.

The CK calculations were performed at the B3LYP level of theory^{26–28} using the 6-31G** split-valence basis set.²⁹ Low-lying isomers, within 50 kcal/mol with respect to the lowest energy isomer, were reoptimized with follow up frequency calculations at the B3LYP level of theory using the 6-311++G** basis set.^{30–33} The final relative energies of the found low-lying isomers were calculated at the CCSD(T)/CBS level by extrapolating CCSD(T)/cc-pvDZ and CCSD(T)/cc-pvTZ^{34–38} to the infinite basis set using the Truhlar formula.^{39,40} Though the CCSD(T)/CBS results may sometimes be less accurate than CCSD(T)/cc-pvTZ results, here we present the results of the CCSD(T)/CBS level of theory for evaluating relative energies of isomers in the $\text{Si}_{6-n}\text{C}_n\text{H}_6$ ($n = 0–6$) series. The relative energies at B3LYP/6-311++G**, CCSD(T)/cc-pvDZ, CCSD(T)/cc-pvTZ, and CCSD(T)/CBS for all studied isomers can be found in the Supporting Information.

A chemical bonding analysis was performed using adaptive natural density partitioning (AdNDP) recently proposed by Zubarev and Boldyrev^{41,42} and natural bond orbital (NBO) analysis developed by Weinhold.^{43,44} The AdNDP approach leads to partitioning of the charge density into elements with the lowest possible number of atomic centers per electron pair: n -center, two-electron ($nc-2e$) bonds, including core electrons, lone pairs, $2c-2e$ bonds, etc. If some part of the density cannot be localized in this manner, it is represented using completely delocalized objects, similar to canonical MOs, naturally incorporating the idea of the completely delocalized bonding. Thus, AdNDP achieves a seamless description of different types of chemical bonds. The density matrix in the basis of the natural atomic orbitals as well as the transformation between atomic orbital and natural atomic orbital basis sets was generated at the B3LYP/6-31G** level of theory by means of the NBO 3.1 code⁴⁵ incorporated into Gaussian 09. It is known that the results of the NBO and AdNDP analysis do not generally depend on the quality of the basis set, so the choice of the level of theory for the AdNDP analysis is adequate. All ab initio calculations were done using the Gaussian 09 program.⁴⁶ AdNDP calculations were performed using the program written by Zubarev. Molecular structure visualization was performed with the Chemcraft⁴⁷ and Molekel 5.4.0.8⁴⁸ programs.

■ RESULTS AND DISCUSSION

In the current article we investigated two transitions in the $\text{Si}_{6-n}\text{C}_n\text{H}_6$ ($n = 0–6$) series upon replacing silicon atoms by carbon atoms. Our first goal was to track where the pseudo-Jahn–Teller effect, responsible for the distortion of planar silabenzene structures is completely suppressed, and the silabenzenes become local minima. Then, we moved on to determination at what n the planar silabenzene isomers become global minimum structures.

Si₆H₆ Isomers. In spite of the fact that five isomers for C₆H₆ stoichiometry: benzene, benzvalene, Dewar-benzene, prismane, and bicycloprenyl have been isolated and well-known,^{49–52} only the hexasilaprismane (structure I.18 ($D_{3h}, ^1\text{A}_1'$), Figure 2) derivative with six tetracoordinate sp³ Si atoms was synthesized until recently. In 2010 K. Abersfelder et al.⁵³ experimentally obtained the tricyclic hexasilabenzene isomer (Si_6R_6 with R = 2,4,6-iPr₃C₆H₂). This compound was reported as stable and according to X-ray crystallography it has a chairlike tricyclic silicon frame. One year later, the same authors isolated and characterized an aryl-substituted version of the global minimum (structure I.1 ($C_{2v}, ^1\text{A}_1$), Figure 2) on the Si₆H₆ potential energy surface.²¹ Hence, three isomers of Si₆H₆ were synthesized to present day.

In our search for the global minimum structure of Si₆H₆ all low-lying isomers revealed by the CK program (at B3LYP/6-31G*) were reoptimized at B3LYP/6-311++G** and obtained geometries were used for single point energy calculations at CCSD(T)/cc-vDZ, CCSD(T)/cc-pvTZ, and CCSD(T)/CBS (see Supporting Information, Figure S1). Our results for Si₆H₆ are in accordance with calculations reported by Moteki et al.²⁰ The most stable isomer on the Si₆H₆ PES is structure I.1, with the third lowest isomer (structure I.3, Figure 2) lying 17.7 kcal/mol above the global minimum. The D_{6h} benzene-like planar structure I.33 (Figure 1) is not a minimum but is a first-order saddle point. Geometry optimization along the imaginary frequency mode leads to distorted chairlike isomer I.32. Planar hexasilabenzene is 51.5 kcal/mol higher in energy than the global minimum I.1 according to our calculations.

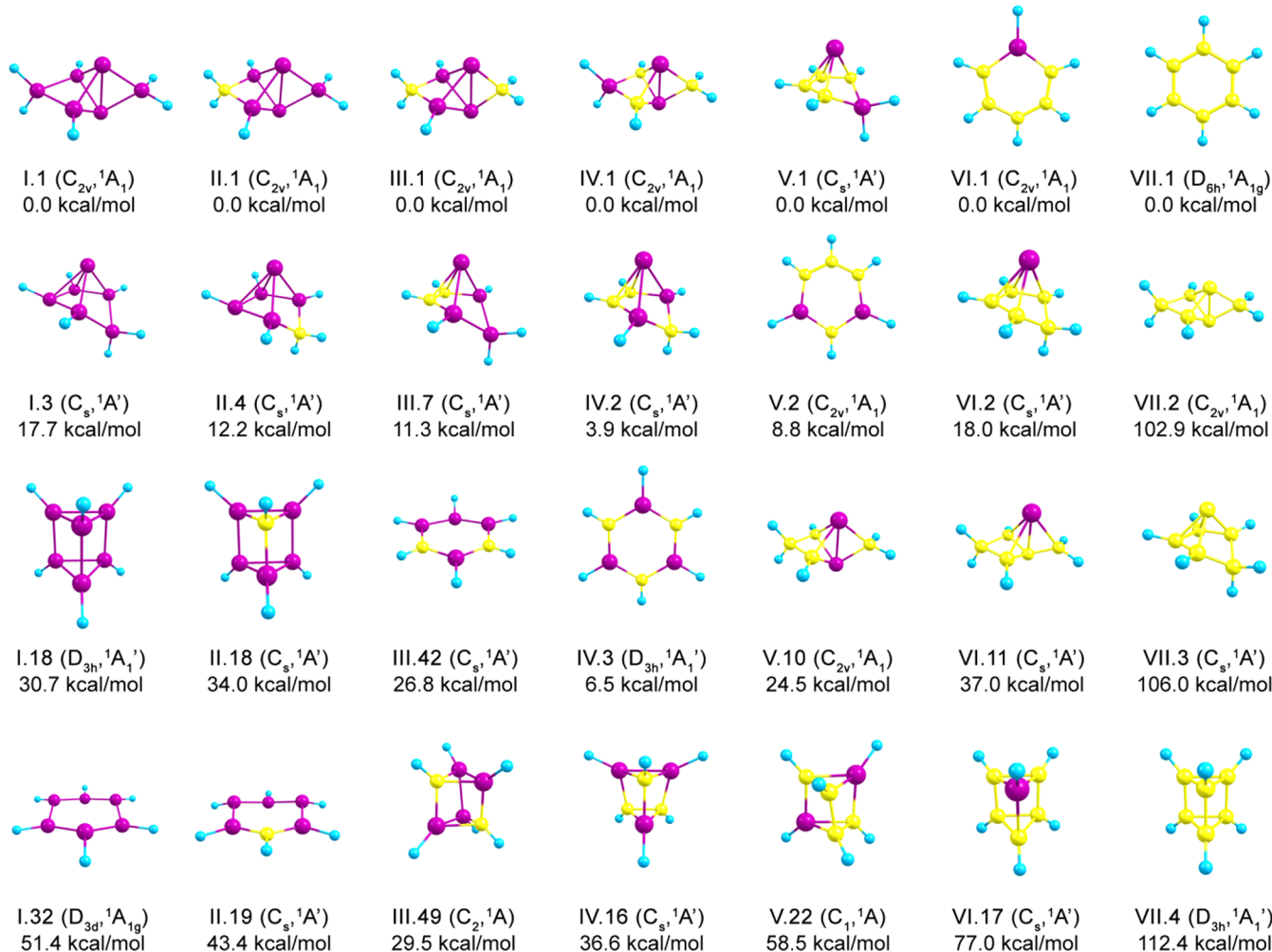


Figure 2. Representative optimized isomers of each species in the $\text{Si}_{6-n}\text{C}_n\text{H}_6$ ($n = 0–6$) series, their point group symmetries, spectroscopic states, and ZPE (B3LYP/6-311++G**) corrected relative energies (CCSD(T)/CBS//B3LYP/6-311++G**). Here and elsewhere the yellow, violet, and blue spheres represent carbon, silicon, and hydrogen atoms, respectively.

The deviation from planarity in hexasilabenzene is caused by the only source of instability of high-symmetry configurations of polyatomic systems, namely, the Jahn–Teller vibronic coupling,^{54,55} the pseudo-Jahn–Teller (PJT) effect to be exact in this case. The distortion of the structure I.33 into the structure I.32 along the b_{2g} mode occurs due to vibronic coupling of HOMO (e_{1g}) and LUMO+2 (e_{2g}). The product of their symmetries contains the symmetry of the imaginary mode (b_{2g}):

$$e_{1g} \otimes e_{2g} = b_{1g} \oplus b_{2g} \oplus e_{1g} \quad (1)$$

Hence, the symmetry rule⁵⁶ for the PJT effect is satisfied as is the second condition:⁵⁶ the symmetry of the imaginary mode (b_{2g}) of the D_{6h} structure corresponds to the symmetric (a_{1g}) mode in the distorted D_{3d} isomer. The HOMO and LUMO+2 gap is 9.78 eV (HF/cc-pvTZ//B3LYP/6-311++G**). The other two closest in energy OMO–UMO pairs [HOMO–1(a_{2u})–LUMO+3(b_{1u}) and HOMO–4(e_{1u}) – LUMO (e_{2u})] corresponding to the symmetry rule, have significantly larger energy gaps: 12.69 and 13.30 eV, respectively. Evidently, the 9.78 eV OMO–UMO gap is small enough to cause the PJT effect. The chairlike structure I.32 is only 2.0 kcal/mol lower (B3LYP/6-311++G**) than planar structure I.33 after zero-point energy correction. It is worthy to notice that

hexasilabenzene is aromatic,¹⁸ but aromaticity itself is not sufficient to make the planar geometry stable and deformation occurs due to the PJT effect.

Si_5CH_6 Isomers. Our CK global minimum search for Si_5CH_6 stoichiometry revealed that structure II.1 (Figure 2) is the global minimum. Structure II.1 is very similar to the global minimum structure of Si_6H_6 . The only difference is that one Si is substituted by the C atom. The second lowest isomer of Si_5CH_6 , structure II.2 (Figure S2, Supporting Information), lying 4.9 kcal/mol higher, is a permutational isomer of the global minimum, with one carbon atom located on the opposite side. Four representative isomers of Si_5CH_6 are shown in Figure 2. The benzene-like structure II.20 (Figure S2, Supporting Information) is 43.9 kcal/mol higher in energy. Again, as it was in the case of hexasilabenzene, monosubstituted Si_6H_6 is a saddle point, but with two imaginary frequency modes [$\omega_1(b_1) = 140.4\text{ cm}^{-1}$ and $\omega_2(a_2) = 43.2\text{ cm}^{-1}$]. The PJT effect is responsible for the two imaginary frequency modes (b_1 and a_2) in the planar C_{2v} structure. Optimization of Si_5CH_6 along the b_1 and a_2 imaginary vibrational modes leads to the C_s structure. Two OMO–UMO pairs giving the b_1 symmetry as a direct product of their symmetries (eqs 2 and 3) are HOMO–1(b_1)–LUMO+1(a_1) and HOMO(a_2)–LUMO+3(b_2) with the energy

gaps of 10.08 and 9.67 eV (HF/cc-pvTZ//B3LYP/6-311++G**), respectively.

$$b_1 \otimes a_1 = b_1 \quad (2)$$

$$a_2 \otimes b_2 = b_1 \quad (3)$$

The direct products of the symmetries of HOMO(a_2)–LUMO+2(a_1) as well as HOMO–2(b_2)–LUMO(b_1) (energy gaps are 9.01 and 10.57 eV, respectively) are a_2 :

$$a_2 \otimes a_1 = a_2 \quad (4)$$

$$b_2 \otimes b_1 = a_2 \quad (5)$$

The symmetries of two imaginary modes in the C_{2v} structure (b_1 and a_2) correspond to the totally symmetric mode a' in the distorted structure II.19 ($C_s, ^1A'$) (Figure 2). Thus, both PJT conditions are met. Substitution of one Si atom in hexasilabenzene leads to higher OMO–UMO gaps in Si_5CH_6 , but the increased gaps are not large enough to prevent orbital coupling and kill the PJT effect.

$\text{Si}_4\text{C}_2\text{H}_6$ Isomers. The CK search of the $\text{Si}_4\text{C}_2\text{H}_6$ species revealed that the potential energy surface has more low-lying structures than that of Si_6H_6 and Si_5CH_6 . We found many structures that are similar to Si_6H_6 and Si_5CH_6 isomers, but with two carbons in the skeleton. The global minimum is the C_{2v} structure III.1 (Figure 2). Prismane structure III.49 is now higher than the benzene-like structure III.43 (Figure S3, Supporting Information) on 2.8 kcal/mol (CCSD(T)/CBS//B3LYP/6-311++G**). Of the three benzene-like isomers, only the 1,2,4,5-isomer (structure III.52 ($D_{2h}, ^1A_g$), Figure S3, Supporting Information) has a planar ground state, but it is the highest among all benzene-like isomers of $\text{Si}_4\text{C}_2\text{H}_6$. The 1,2,3,5-isomer III.43 is 8.9 kcal/mol lower than the 1,2,3,4-isomer III.51 ($C_{2v}, ^1A_1$) (Figure S3, Supporting Information); however, both of them are just first-order saddle points with imaginary frequency modes of $\omega(b_1) = 151.2i \text{ cm}^{-1}$ and $\omega(a_2) = 184.2i \text{ cm}^{-1}$, respectively. The b_1 imaginary frequency mode in the C_{2v} structure III.43 is again a consequence of the PJT effect, but the a_2 mode is now real. Optimization of the structure along b_1 imaginary mode leads to the C_s structure III.42 (Figure 2). The direct product of HOMO(b_1) and LUMO+2(a_1) yields b_1 , which is the symmetry of the imaginary mode:

$$b_1 \otimes a_1 = b_1 \quad (6)$$

The HOMO and LUMO+2 gap is 9.77 eV (HF/cc-pvTZ//B3LYP/6-311++G**). The closest in energy OMO–UMO pairs, giving a_2 as a direct product of symmetries, HOMO(b_1)–LUMO+3(b_2) and HOMO–1(a_2)–LUMO+2(a_1), have energy gaps of 10.46 and 11.32 eV, respectively. Interestingly, this small increase in the UMO–OMO gap is enough to suppress the PJT effect along the a_2 mode.

Structure III.51 (the 1,2,3,4-isomer of $\text{Si}_4\text{C}_2\text{H}_6$) undergoes the PJT distortion along the a_2 imaginary frequency mode into the twisted C_2 structure III.50 because of interaction of HOMO(a_2) with LUMO+2(a_1) (the HOMO–LUMO+2 gap, computed at HF/cc-pvTZ//B3LYP-6-311++G**, is 9.24 eV).

Finally, for the D_{2h} structure III.52 (the 1,2,4,5-isomer of $\text{Si}_4\text{C}_2\text{H}_6$) two lowest vibrational frequencies ($\omega_1(b_{2g}) = 73.5 \text{ cm}^{-1}$ and $\omega_2(a_u) = 73.9 \text{ cm}^{-1}$) have a small but real values for both frequencies. The gap between the closest OMO–UMO pair [HOMO(b_{1g})–LUMO+3(b_{3g})] leading to b_{2g} symmetry is 9.93 eV and the OMO–UMO pair [HOMO(b_{1g})–LUMO

+4(b_{1u})] leading to a_u symmetry is 10.15 eV. Obviously, the OMO–UMO gap is now higher than in the two other cases and that is enough to kill the PJT effect in this case.

$\text{Si}_3\text{C}_3\text{H}_6$ Isomers. From our CK search for the global minimum structure of $\text{Si}_3\text{C}_3\text{H}_6$ stoichiometry, we found that again structure IV.1 (Figure 2) similar to the global minimum structures of Si_6H_6 – $\text{Si}_4\text{C}_2\text{H}_6$ is the lowest energy isomer on the $\text{Si}_3\text{C}_3\text{H}_6$ PES. The prismane isomer IV.16, lying 36.6 kcal/mol above the global minimum, is now the least stable of the considered structures shown in Figure 2. Of the three planar isomers, 1,3,5-trisilabenzene (structure IV.3, Figure 2) is the lowest one, and it has been thoroughly studied theoretically.^{57–60} Moreover, in 2003 it was synthesized as a ligand according to the experimental reports.⁶¹ The 1,3,5-trisilabenzene is the global minimum (at B3LYP/6-311++G**//B3LYP/6-311++G**, Figure S4, Supporting Information); however, our most accurate single-point calculations at CCSD(T)/CBS//B3LYP/6-311++G** showed that planar structure IV.3 is the third lowest isomer, following the isomers IV.2 and IV.1, respectively (Figure 2). We can see that in our $\text{Si}_{6-n}\text{C}_n\text{H}_6$ series at $n = 3$, the energy difference between three-dimensional and planar structures is not large anymore (6.5 kcal/mol).

The lowest frequency [$\omega(e'') = 211.7 \text{ cm}^{-1}$] for the planar D_{3h} structure IV.3 is real. The gap (HF/cc-pvTZ//B3LYP/6-311++G**) between the closest OMO–UMO pair [HOMO–(e'')–LUMO+1(a_1')] leading to e'' symmetry is now as large as 11.91 eV. Hence, a substantial increase in the OMO–UMO gap is responsible for quenching the PJT effect. The experimental observation of planarity of 1,3,5-trisilabenzene also proves the point that the PJT is completely suppressed at $n = 3$.

However, the other two planar isomers: 1,2,3-trisilabenzene IV.9 and 1,3,5-trisilabenzene IV.14 (Figure S4, Supporting Information), lying 19.8 and 23.5 kcal/mol higher than the global minimum, are first-order saddle points with small out-of-plane imaginary frequencies of 84.5i and 66.0i cm^{-1} , respectively. Geometry optimization along b_1 (structure IV.9) and a'' (structure IV.14) imaginary frequency modes would give the C_s structure IV.11 and the C_1 structure IV.15 (Figure S4, Supporting Information), accordingly. The difference in total energies between the saddle-point planar structures and the corresponding C_s and C_1 structures is smaller than the difference in zero-point energy corrections for these structures, with the zero-point energy for the C_s and C_1 isomers being slightly larger. Thus, after zero-point energy corrections the planar structures of 1,2,3-trisilabenzene IV.9 and 1,3,5-trisilabenzene IV.14 are of lower energy than the corresponding C_s IV.11 and C_1 IV.15 structures.

$\text{Si}_2\text{C}_4\text{H}_6$ Isomers. According to the results of our CK search, structure V.1 is the global minimum and it is analogous to structures I.3, II.4, III.7, and IV.2 in the $\text{Si}_{6-n}\text{C}_n\text{H}_6$ series. Structure V.10, analogs of which have been global minima until $n = 4$ in the series, is 24.5 kcal/mol above the global minimum. Prismane isomer V.22 is now 58.5 kcal/mol higher than the global minimum structure. Of the three planar isomers, structure V.2 is the most stable, with the C_{2v} structure V.3 and D_{2h} structure V.7 (Figure S5, Supporting Information) being second and third planar lowest-lying structures, respectively. Again, planar structure V.2 of disilabenzene is the global minimum at B3LYP/6-311++G**//B3LYP/6-311++G** but is only the second lowest isomer according to the CCSD(T)/CBS//B3LYP/6-311++G** level of theory.

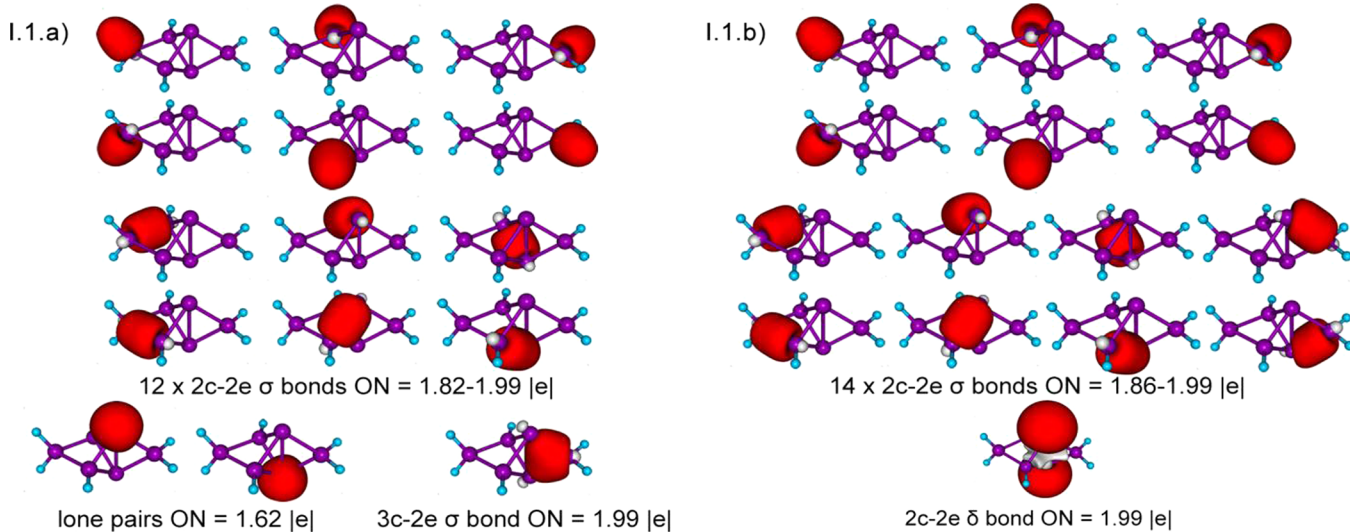


Figure 3. Two representations of chemical bonding patterns of the I.1 global minimum structure revealed by the AdNDP.

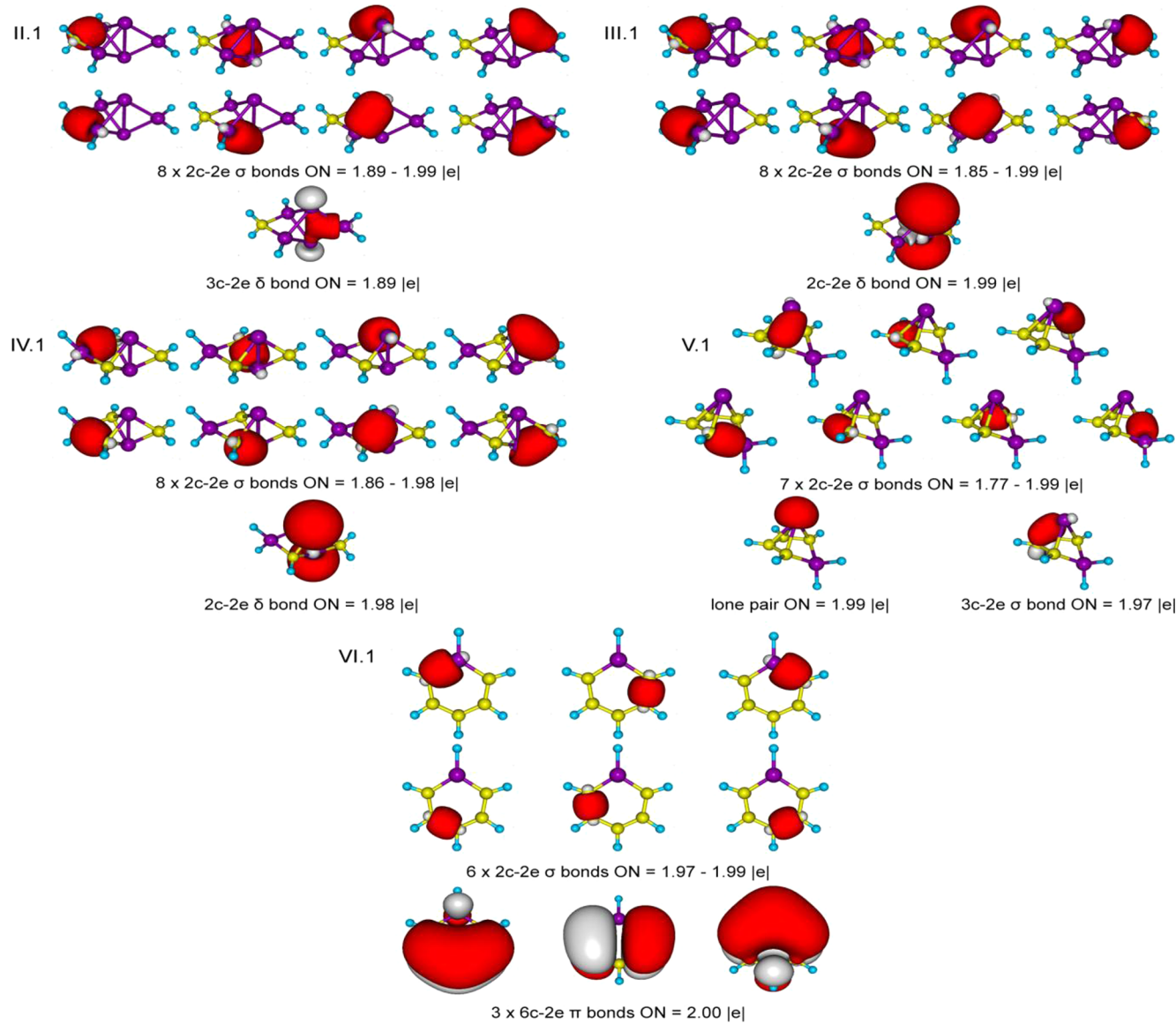


Figure 4. Chemical bonding patterns of the II.1, III.1, IV.1, V.1, and VI.1 global minimum structures revealed by the AdNDP.

A lot of theoretical works were devoted to the investigation of disilabenzenes.^{60,62,63} Our values of the relative energies are in agreement with those obtained by Deva Priyakumar et al.⁶³ First experimental isolation of disilabenzenes derivative was reported in 1987, when hexamethyl-substituted 1,4-disilabenzene has been synthesized.⁶⁴ In 2001 Dysard et al.⁶⁵ experimentally proved the existence of silabenzene and 1,4-disilabenzene as ruthenium complexes.

SiC₅H₆ Isomers. For the SiC₅H₆ stoichiometry we found that monosilabenzene VI.1 is the global minimum with the second isomer VI.2 lying significantly higher (the difference in energy is 18.0 kcal/mol at CCSD(T)/CBS//B3LYP/6-311++G**). The prismane structure VI.17 is higher in energy than the global minimum by 77.0 kcal/mol. The selected lowest isomers are presented in Figure 2. A more extensive set of alternative structures is given in the Supporting Information (Figure S6).

According to our systematic computational study, the 3D–2D transition occurs only at $n = 5$, where planar monosilabenzene structure becomes much more stable than the three-dimensional structures.

A large number of theoretical studies were done on monosilabenzene before its spectral data and matrix isolation.^{66–69} The derivative of monosilabenzene (2,6-bis(trimethylsilyl)-1,4-di(*tert*-butyl)monosilabenzene) is known to be stable in solution.⁷⁰

Our results regarding Si₆H₆, Si₅CH₆, Si₄C₂H₆, Si₃C₃H₆, Si₂C₄H₆, and SiC₅H₆ silabenzenes are generally in agreement with calculations made by Baldridge et al.,⁶⁰ however, we were not able to find any theoretical or experimental data concerning Si₅CH₆, Si₄C₂H₆, and Si₃C₃H₆ isomers in the literature.

C₆H₆ Isomers. The aforementioned systematic computational study¹ of the C₆H₆ isomers revealed 215 minimum energy structures, with 84 structures being within 100 kcal/mol in energy relative to the benzene global minimum structure. Benzene is the most stable isomer. In this article, we present four isomers of C₆H₆ in Figure 2. According to our calculations, prismane VII.4 is higher in energy than the third isomer (VII.3) and the second isomer (VII.2), respectively. The relative energies of the presented structures are given at the CCSD(T)/CBS//B3LYP/6-311++G** level of theory.

Chemical Bonding Pictures Revealed by the AdNDP. To interpret our results from the chemical bonding point of view, we performed the AdNDP analysis for the global minimum structures. The results of our analysis for these structures are shown in Figures 3 and 4.

There are two interpretations of chemical bonding for the Si₆H₆ global minimum structure (I.1) (Figure 3). According to the first picture (Figure 3, I.1.a), the AdNDP analysis revealed six two-center, two-electron (2c–2e) Si–H σ bonds, six 2c–2e Si–Si σ bonds, all with occupation numbers (ON) ranging from 1.82 lel to 1.99 lel; two lone pairs with ON = 1.62 lel on two silicon atoms, and one three-center, two electron (3c–2e) σ bond (ON = 1.99 lel).

To improve this zero-order chemical bonding model, we need to accept all bonding elements which have ON close to 2.00 lel and allow the bonding elements with low occupation numbers to be delocalized over larger number of atoms. In other words, in our new AdNDP search we accepted bonding patterns with ON higher than 1.80 lel. Therefore, the AdNDP revealed six 2c–2e Si–H σ bonds, eight 2c–2e Si–Si σ bonds (all with ON = 1.86–1.99 lel), and one δ bond between two silicon atoms (Figure 3, I.2.b). Hence, we offer two chemical

bonding pictures that can describe chemical bonding in the Si₆H₆ global minimum structure.

We also performed the AdNDP analysis for the Si₅CH₆ (II.1), Si₄C₂H₆ (III.1), Si₃C₃H₆ (IV.1), Si₂C₄H₆ (V.1), and SiC₅H₆ (VI.1) global minimum structures. Results of these analyses are presented in Figure 4 (for Si₅CH₆, Si₄C₂H₆, and Si₃C₃H₆ global minimum structures, accepted bonding patterns with ON higher than 1.80 lel were chosen).

For the Si₅CH₆ global minimum structure II.1, we found six 2c–2e Si–H σ bonds with ON = 1.98–1.99 lel (not shown in Figure 4), eight 2c–2e Si–Si σ bonds (ON = 1.89–1.99 lel), and one 3c–2e Si–Si δ bond (ON = 1.98 lel). The Si₄C₂H₆ global minimum structure III.1 has six 2c–2e Si–H σ bonds with ON = 1.98–1.99 lel (not shown in Figure 4), eight 2c–2e Si–Si σ bonds (ON = 1.85–1.99 lel), and one 2c–2e Si–Si δ bond (ON = 1.99 lel). The Si₃C₃H₆ global minimum structure IV.1 has a chemical bonding picture similar to that of III.1: six 2c–2e Si–H σ bonds with ON = 1.98–1.99 lel (not shown in Figure 4), eight 2c–2e Si–Si σ bonds (ON = 1.86–1.98 lel), and one 2c–2e Si–Si δ bond (ON = 1.98 lel). For the Si₂C₄H₆ global minimum structure V.1, the AdNDP revealed six 2c–2e Si–H σ bonds with ON = 1.98–1.99 lel (not shown in Figure 4), seven 2c–2e Si–Si σ bonds (ON = 1.77–1.99 lel), one lone pair on silicon atom with ON = 1.99 lel, and one 3c–2e Si–Si σ bond (ON = 1.97 lel). The planar monosilabenzene global minimum structure VI.1 has six 2c–2e Si–H σ bonds with ON = 1.98–2.00 lel (not shown in Figure 4), six 2c–2e Si–Si σ bonds with occupation numbers being close to ideal values of 2.00 lel; and three six-center two electron (6c–2e) Si–Si π bonds (ON = 2.00 lel) confirming the presence of π -aromaticity in this molecule.

CONCLUSIONS

We presented a systematic study of the Si_{6-n}C_nH₆ ($n = 0–6$) series. We performed unbiased CK global minimum and low-lying isomers search for the Si₆H₆, Si₅CH₆, Si₄C₂H₆, Si₃C₃H₆, Si₂C₄H₆, and SiC₅H₆ species at the B3LYP/6-31G** level of theory. The lowest isomers were recalculated at the CCSD(T)/CBS//B3LYP/6-311++G** level of theory. We found that the OMO–UMO gap between MOs involved in the PJT effect is increasing with substitution of the Si atoms by the C atoms, which gradually leads to the suppression of the PJT effect in 1,3,5-trisilabenzene. Recently, it was shown in the C_xH_xP_{6-x} ($x = 0–6$)⁷¹ and C_xH_xP_{4-x} ($x = 0–4$)⁷² series that isolobal substitution of an atom or a group by a more electronegative atom or group can be considered as a new mechanism for the suppression of the PJT effect.

As we can see from our chemical bonding analysis, the most stable structure VI.1 for SiC₅H₆ is aromatic. The NICS values, obtained by Baldridge et al.⁶⁰ show that aromaticity increases with decreasing number of silicon atoms along the silabenzenes series. However, the transition from three-dimensional structures to planar structures occurs only at $n = 5$ in the Si_{6-n}C_nH₆ ($n = 0–6$) series. Thus, relating stability with aromaticity in silicon–carbon compounds could be risky. According to our results there are also other reasons for the switch in the relative stabilities in the considered series upon the substitution of silicon atoms by carbon atoms. The environment in which the Si atoms are located and the strain energy in the skeleton of silicon structures are some factors in explaining the observed stabilities. The isomer, in which all silicon atoms are tetracoordinated was found to be more stable among other isomers of the Si₆H₆, Si₅CH₆, Si₄C₂H₆, and

$\text{Si}_3\text{C}_3\text{H}_6$ stoichiometries. Hence, the silicon atoms would prefer to be tetracoordinated and form three-dimensional structures that can be explained by the weak π -bonding of silicon atoms with carbon atoms or with another Si. Our theoretical study may be useful for understanding geometry, properties, and nature of the Si–C compounds and may become a guiding tool for experimental research in this area.

■ ASSOCIATED CONTENT

Supporting Information

Geometric structures and relative energies (CCSD(T)/CBS, CCSD(T)/cc-pVTZ, CCSD(T)/cc-pVQZ, and B3LYP/6-311+G**, all at B3LYP/6-311++G** geometries) of all studied isomers. Cartesian coordinates of global minimum structures (B3LYP/6-311++G**) for all considered stoichiometries. This material is available free of charge via the Internet at <http://pubs.acs.org>.

■ AUTHOR INFORMATION

Corresponding Author

*E-mail: a.i.boldyrev@usu.edu.

Notes

The authors declare no competing financial interest.

■ ACKNOWLEDGMENTS

The National Science Foundation (Grant CHE-1057746) supported this work. Cluster time and other computational resources from the Center for High Performance Computing at Utah State University are gratefully acknowledged. The computational resources of the 64 node Wasatch cluster were funded by the National Institute of Food and Agriculture, U.S. Department of Agriculture, through the High Performance Computing Utah grant.

■ REFERENCES

- (1) Dinadayalane, T. C.; Priyakumar, U. D.; Sastry, G. N. *J. Phys. Chem. A* **2004**, *108*, 11433.
- (2) Malrieu, J. P.; Trinquier, G. *J. Am. Chem. Soc.* **1989**, *111*, 5916.
- (3) Jacobsen, H.; Ziegler, T. *J. Am. Chem. Soc.* **1994**, *116*, 3667.
- (4) Scherer, O. J.; Sitzmann, H.; Wolmershauser, G. *Angew. Chem., Int. Ed.* **1985**, *24*, 351.
- (5) Nagase, S.; Kobayashi, K.; Takagi, N. *J. Organomet. Chem.* **2000**, *611*, 264.
- (6) Frenking, G.; Krapp, A.; Nagase, S.; Takagi, N.; Sekiguchi, A. *ChemPhysChem.* **2006**, *7*, 799.
- (7) Power, P. P. *Chem. Rev.* **1999**, *99*, 3463.
- (8) Sari, L.; McCarthy, M. C.; Schaefer, H. F., III; Thaddeus, P. *J. Am. Chem. Soc.* **2003**, *125*, 11409.
- (9) Binkley, J. S. *J. Am. Chem. Soc.* **1984**, *106*, 603.
- (10) Nagase, S.; Nakano, M. *Angew. Chem., Int. Ed. Engl.* **1988**, *27*, 1081.
- (11) Yates, B. F.; Schaefer, H. F., III. *Chem. Phys. Lett.* **1989**, *155*, 563.
- (12) Kosa, M.; Karni, M.; Apeloig, Y. *J. Chem. Theory Comput.* **2006**, *2*, 956.
- (13) Sax, A.; Janoschek, R. *Angew. Chem., Int. Ed. Engl.* **1986**, *25*, 651.
- (14) Nagase, S.; Teramae, H.; Kudo, T. *J. Chem. Phys.* **1987**, *86*, 4513.
- (15) Zdetsis, A. D. *J. Chem. Phys.* **2007**, *214306*.
- (16) Santos, J. C.; Contreras, M.; Merino, G. *Chem. Phys. Lett.* **2010**, *496*, 172.
- (17) Nagase, S.; Kudo, T.; Aoki, M. *J. Chem. Soc., Chem. Commun.* **1985**, 1121.
- (18) Schleyer, P. v. R.; Jiao, H.; Hommes, N. J. R. v. E.; Malkin, V. G.; Malkina, O. N. *J. Am. Chem. Soc.* **1997**, *119*, 12669.
- (19) Zhao, M.; Gimarc, B. M. *Inorg. Chem.* **1996**, *35*, 5378.
- (20) Moteki, M.; Maeda, S.; Ohno, K. *Organometallics* **2009**, *28*, 2218.
- (21) Abersfelder, K.; White, A. J. P.; Berger, R. J. F.; Rzepa, H. S.; Scheschke, D. *Angew. Chem., Int. Ed.* **2011**, *50*, 7936.
- (22) Sergeeva, A. P.; Averkiev, B. B.; Zhai, H. J.; Boldyrev, A. I.; Wang, L. S. *J. Chem. Phys.* **2011**, *134*, 224304.
- (23) Schlegel, H. B. *J. Comput. Chem.* **1982**, *3*, 214.
- (24) Wang, X. B.; Nicholas, J. B.; Wang, L. S. *J. Chem. Phys.* **2000**, *113*, 10837.
- (25) Wang, X. B.; Sergeeva, A. P.; Yang, J.; Xing, X. P.; Boldyrev, A. I.; Wang, L. S. *J. Phys. Chem. A* **2009**, *113*, 5567.
- (26) Becke, A. D. *J. Chem. Phys.* **1993**, *98*, 5648.
- (27) Vosko, S. H.; Wilk, L.; Nusair, M. *Can. J. Phys.* **1980**, *58*, 1200.
- (28) Lee, C.; Yang, W.; Parr, R. G. *Phys. Rev. B: Condens. Matter* **1988**, *37*, 785.
- (29) Binkley, J. S.; Pople, J. A.; Hehre, W. J. *J. Am. Chem. Soc.* **1980**, *102*, 939.
- (30) Rassolov, V. A.; Ratner, M. A.; Pople, J. A.; Redfern, P. C.; Curtiss, L. A. *J. Comput. Chem.* **2001**, *22*, 976.
- (31) Gordon, M. S.; Binkley, J. S.; Pople, J. A.; Pietro, W. J.; Hehre, W. J. *J. Am. Chem. Soc.* **1982**, *104*, 2797.
- (32) Pietro, W. J.; Frandl, M. M.; Hehre, W. J.; Defrees, D. J.; Pople, J. A.; Binkley, J. S. *J. Am. Chem. Soc.* **1982**, *104*, 5039.
- (33) Clark, T.; Chandrasekhar, J.; Spitznagel, G. W.; Schleyer, P. v. R. *J. Comput. Chem.* **1983**, *4*, 294.
- (34) Woon, D. E.; Dunning, T. H., Jr. *J. Chem. Phys.* **1993**, *98*, 1358.
- (35) Kendall, R. A.; Dunning, T. H.; Harrison, R. J. *J. Chem. Phys.* **1992**, *96*, 6796.
- (36) Dunning, T. H. *J. Chem. Phys.* **1989**, *90*, 1007.
- (37) Peterson, K. A.; Woon, D. E.; Dunning, T. H. *J. Chem. Phys.* **1994**, *100*, 7410.
- (38) Wilson, A.; van Mourik, T.; Dunning, T. H. *THEOCHEM* **1997**, *388*, 339.
- (39) Truhlar, D. G. *Chem. Phys. Lett.* **1998**, *294*, 45.
- (40) Fast, P. L.; Sanchez, M. L.; Truhlar, D. G. *J. Chem. Phys.* **1999**, *111*, 2921.
- (41) Zubarev, D. Yu.; Boldyrev, A. I. *Phys. Chem. Chem. Phys.* **2008**, *10*, 5207.
- (42) Zubarev, D. Yu.; Robertson, N.; Domin, D.; McClean, J.; Wang, J. H.; Lester, W. A.; Whitesides, R.; You, X. Q.; Frenklach, M. *J. Phys. Chem. C* **2010**, *114*, 5429.
- (43) Foster, J. P.; Weinhold, F. *J. Am. Chem. Soc.* **1980**, *102*, 7211.
- (44) Reed, A. E.; Curtiss, L. A.; Weinhold, F. *Chem. Rev.* **1988**, *88*, 899.
- (45) Glendening, E. D.; Reed, A. E.; Carpenter, J. E.; Weinhold, F. NBO, version 3.1.
- (46) Frisch, M. J.; Trucks, G. W.; Schlegel, H. B.; Scuseria, G. E.; Robb, M. A.; Cheeseman, J. R.; Scalmani, G.; Barone, V.; Mennucci, B.; Petersson, G. A.; Nakatsuji, H.; Caricato, M.; Li, X.; Hratchian, H. P.; Izmaylov, A. F.; Bloino, J.; Zheng, G.; Sonnenberg, J. L.; Hada, M.; Ehara, M.; Toyota, K.; Fukuda, R.; Hasegawa, J.; Ishida, M.; Nakajima, T.; Honda, Y.; Kitao, O.; Nakai, H.; Vreven, T.; Montgomery, J. A., Jr.; Peralta, J. E.; Ogliaro, F.; Bearpark, M.; Heyd, J. J.; Brothers, E.; Kudin, K. N.; Staroverov, V. N.; Kobayashi, R.; Normand, J.; Raghavachari, K.; Rendell, A.; Burant, J. C.; Iyengar, S. S.; Tomasi, J.; Cossi, M.; Rega, N.; Millam, N. J.; Klene, M.; Knox, J. E.; Cross, J. B.; Bakken, V.; Adamo, C.; Jaramillo, J.; Gomperts, R.; Stratmann, R. E.; Yazev, O.; Austin, A. J.; Cammi, R.; Pomelli, C.; Ochterski, J. W.; Martin, R. L.; Morokuma, K.; Zakrzewski, V. G.; Voth, G. A.; Salvador, P.; Dannenberg, J. J.; Dapprich, S.; Daniels, A. D.; Farkas, O.; Foresman, J. B.; Ortiz, J. V.; Cioslowski, J.; Fox, D. J. *Gaussian 09*, Revision B.01; Gaussian, Inc.: Wallingford, CT, 2010.
- (47) <http://www.chemcraftprog.com>.
- (48) Varetto, U. *Molekel*, version 5.4.0.8; Swiss National Supercomputing Centre: Manno, Switzerland, 2009.
- (49) Foote, J. K.; Mallon, M. H.; Pitts, J. N. *J. Am. Chem. Soc.* **1966**, *88*, 3698.
- (50) van Tamelen, E. E.; Pappas, S. P. *J. Am. Chem. Soc.* **1963**, *85*, 3297.

- (51) Katz, T. J.; Acton, N. *J. Am. Chem. Soc.* **1973**, *95*, 2738.
(52) Billups, W. E.; Haley, M. M. *Angew. Chem., Int. Ed. Engl.* **1989**, *28*, 1711.
(53) Abersfelder, K.; White, A.; Rzepa, H.; Scheschkewitz, D. *Science* **2010**, *327*, 564.
(54) Bersuker, I. B. *Chem. Rev.* **2001**, *101*, 1067.
(55) Bersuker, I. B. In *The Jahn-Teller Effect*; Cambridge University Press: Cambridge, U.K., 2006.
(56) Pearson, R. G. *Proc. Natl. Acad. Sci. U. S. A.* **1975**, *72*, 2104.
(57) Matsunaga, N.; Gordon, M. S. *J. Am. Chem. Soc.* **1994**, *116*, 11407.
(58) Matsunaga, T. R.; Cundari, T. R.; Schmidt, M. W.; Gordon, M. *S. Theor. Chim. Acta* **1992**, *83*, 57.
(59) Pipek, J.; Mezey, P. G. *J. Chem. Phys.* **1989**, *90*, 4916.
(60) Baldridge, K. K.; Uzan, O.; Martin, J. M. L. *Organometallics* **2000**, *19*, 1477.
(61) Bjarnason, A.; Arnason, I. *Angew. Chem., Int. Ed. Engl.* **1992**, *31*, 1633.
(62) Baldridge, K. K.; Gordon, M. S. *J. Am. Chem. Soc.* **1984**, *106*, 369.
(63) Deva Priyakumar, U.; Saravanan, D.; Narahari Sastry, G. *Organometallics* **2002**, *21*, 4823.
(64) Welsh, K. M.; Rich, J. D.; West, R. J. *Organomet. Chem.* **1987**, *325*, 105.
(65) Dysard, J. M.; Tilley, T. D.; Woo, T. K. *Organometallics* **2001**, *20*, 1195.
(66) Barton, T. J.; Burns, G. T. *J. Am. Chem. Soc.* **1978**, *100*, 5246.
(67) Maier, G.; Mihm, G.; Reisenauer, H. P. *Angew. Chem., Int. Engl. Ed.* **1980**, *19*, 52.
(68) Maier, G.; Mihm, G.; Reisenauer, H. P. *Chem. Ber.* **1982**, *115*, 801.
(69) Solouki, B.; Rosmus, P.; Bock, H.; Maier, G. *Angew. Chem., Int. Ed. Engl.* **1980**, *19*, 51.
(70) Markl, G.; Hofmeister, P. *Angew. Chem., Int. Ed. Engl.* **1979**, *18*, 789.
(71) Galeev, T. R.; Boldyrev, A. I. *Phys. Chem. Chem. Phys.* **2011**, *13*, 20549.
(72) Ivanov, A. S.; Bozhenko, K. V.; Boldyrev, A. I. *J. Chem. Theory Comput.* **2012**, *8*, 135.